

DYNAMICAL SIGNALS IN FRAGMENTATION  
REACTIONS: TIME SCALE DETERMINATION FROM  
THREE FRAGMENTS CORRELATIONS BY USING  
THE  $4\pi$  CHIMERA MULTIDETECTOR\*

E. DE FILIPPO<sup>a,b,†</sup>, F. AMORINI<sup>c</sup>, A. ANZALONE<sup>c</sup>, L. AUDITORE<sup>d</sup>, V. BARAN<sup>e,f</sup>  
I. BERCEANU<sup>e</sup>, J. Blicharska<sup>g</sup>, B. BORDERIE<sup>h</sup>, R. BOUGAULT<sup>i</sup>, M. BRUNO<sup>j</sup>  
J. BRZYCHCZYK<sup>k</sup>, G. CARDELLA<sup>a,b</sup>, S. CAVALLARO<sup>c</sup>, M.B. CHATTERJEE<sup>l</sup>  
A. CHBIHI<sup>m</sup>, M. COLONNA<sup>c</sup>, M. D'AGOSTINO<sup>j</sup>, R. DAYRAS<sup>n</sup>, M. DI TORO<sup>c</sup>  
U. EMANUELE<sup>d</sup>, J. FRANKLAND<sup>m</sup>, E. GALICHET<sup>h</sup>, W. GAWLIKOWICZ<sup>k</sup>, E. GERACI<sup>a,b</sup>  
F. GIUSTOLISI<sup>c</sup>, L. GRASSI<sup>a,b</sup>, A. GRZESZCZUK<sup>g</sup>, P. GUAZZONI<sup>o</sup>, D. GUINET<sup>p</sup>  
S. KOWALSKI<sup>g</sup>, E. LA GUIDARA<sup>c</sup>, G. LANZALONE<sup>c</sup>, G. LANZANÒ<sup>a,b</sup>, N. LE NEINDRE<sup>i</sup>  
I. LOMBARDO<sup>c</sup>, C. MAIOLINO<sup>c</sup>, Z. MAJKA<sup>k</sup>, A. PAGANO<sup>a,b</sup>, M. PAPA<sup>a,b</sup>  
M. PETROVICI<sup>e</sup>, E. PIASECKI<sup>q</sup>, S. PIRRONE<sup>a,b</sup>, R. PLANETA<sup>k</sup>, G. POLITI<sup>a,b</sup>, A. POP<sup>e</sup>  
F. PORTO<sup>c</sup>, M.F. RIVET<sup>h</sup>, E. ROSATO<sup>r</sup>, F. RIZZO<sup>c</sup>, P. RUSSOTTO<sup>c</sup>, K. SCHMIDT<sup>g</sup>  
K SIWEK-WILCZYŃSKA<sup>q</sup>, I. SKWIRA<sup>q</sup>, A. SOCHOCKA<sup>k</sup>, A. TRIFIRÒ<sup>d</sup>, M. TRIMARCHI<sup>d</sup>  
G. VERDE<sup>a,b</sup>, M. VIGILANTE<sup>r</sup>, J.P. WIELECZKO<sup>m</sup>, J. WILCZYŃSKI<sup>s</sup>, L. ZETTA<sup>o</sup>  
W. ZIPPER<sup>g</sup>

<sup>a</sup>INFN Sezione di Catania, Italy

<sup>b</sup>Dipartimento di Fisica, Università di Catania, Italy

<sup>c</sup>INFN Lab. Naz. del Sud and Dip. di Fisica, Università di Catania, Italy

<sup>d</sup>INFN, Gr. coll. di Messina and Dip. di Fisica, Università di Messina, Italy

<sup>e</sup>Institute for Physics and Nuclear Engineering, Bucharest, Romania

<sup>f</sup>University of Bucharest, Romania

<sup>g</sup>Institute of Physics, University of Silesia, Katowice, Poland

<sup>h</sup>Institut de Physique Nucléaire, IN2P3-CNRS, Orsay, France

<sup>i</sup>LPC, ENSI Caen and Université de Caen, France

<sup>j</sup>INFN Sez. di Bologna and Dipartimento di Fisica, Università di Bologna, Italy

<sup>k</sup>M. Smoluchowski Institute of Physics, Jagellonian University, Cracow, Poland

<sup>l</sup>Saha Institute of Nuclear Physics, Kolkata, India

<sup>m</sup>GANIL, CEA, IN2P3-CNRS, Caen, France

<sup>n</sup>DAPNIA/SPhN, CEA-Saclay, France

<sup>o</sup>INFN Sez. di Milano and Dipartimento di Fisica, Università di Milano, Italy

<sup>p</sup>IPN, IN2P3-CNRS and Université Claude Bernard, Lyon, France

<sup>q</sup>Institute for Experimental Physics, Warsaw University, Warsaw, Poland

<sup>r</sup>INFN Sez. di Napoli and Dipartimento di Fisica, Università di Napoli, Italy

<sup>s</sup>A. Sołtan Institute for Nuclear Studies, Swierk/Warsaw, Poland

(Received February 4, 2009)

---

\* Presented at the IV Workshop on Particle Correlations and Femtoscopy, Kraków, Poland, September 11–14, 2008.

† Corresponding author: [defilippo@ct.infn.it](mailto:defilippo@ct.infn.it)

For fragments emitted in the reactions  $^{124}\text{Sn} + ^{64}\text{Ni}$  and  $^{112}\text{Sn} + ^{58}\text{Ni}$  at 35 A MeV, isotopic composition and velocity correlations have been studied as a function of the centrality of the collision, using the  $4\pi$  Chimera multidetector. We have investigated the time scale for fragments formation, in order to distinguish between prompt dynamical and sequential statistical emission. Promptly emitted light fragments ( $Z \leq 9$ ) produced in the mid-rapidity domain are characterised by larger  $N/Z$  ratio and stronger angular anisotropies than those produced in sequential statistical emission. Results are compared with stochastic BNV code simulations obtained for primary fragments. Valuable information on the symmetry term of the nuclear equation of state at sub-saturation densities are obtained.

PACS numbers: 25.70.Mn, 25.70.Pq

## 1. Introduction

The study of isospin degree of freedom in nuclear reactions induced by stable or radioactive beams is suited to probe the nuclear equation of state (EOS). In particular, recent investigations have demonstrated a sensitivity of isospin observables to the symmetry energy [1]. In recent years we have undertaken several experiments with the CHIMERA multi-detector [2] designed to explore isospin dynamics from central to peripheral reactions. In this work we illustrate a method, based on fragment–fragment correlations of the three biggest fragments of the detected events, that can provide information upon time-scale and chronology of the emission pattern of nuclear fragments. The analysis is based essentially on the evaluation of final state (Coulomb) interaction between fragments produced in the collisions. We show that the neutron to proton ( $N/Z$ ) ratio can be correlated with fragment emission time. The correlations between fragment kinematical properties (relative velocities, degree of alignment, angular distributions) and their isotopic contents show characteristic shapes that can be reproduced with a “stiff” behaviour of the symmetry energy. The phenomenon is followed as a function of the degree of dissipation of the reaction.

The measurements were performed at the INFN-Laboratorio Nazionale del Sud in Catania using  $^{124}\text{Sn}$  and  $^{112}\text{Sn}$  35 A MeV energy beams delivered by the Superconducting Cyclotron, bombarding respectively  $^{64}\text{Ni}$  and  $^{58}\text{Ni}$  thin targets placed inside the CHIMERA array. Chimera is constituted by 1192 telescopes. Each telescope consists of a planar silicon detector followed by a CsI(Tl) scintillator. 688 detection cells are arranged in nine rings covering the polar angular range between  $1^\circ$  and  $30^\circ$  in a full  $2\pi$  azimuthal symmetry around the beam axis. All the other cells are arranged in a sphere (40 cm radius) covering the backward angles around the target. Data presented here refers to a configuration in which the sphere section was not

present in the experiment. More details of identification techniques can be found elsewhere [3]. Only data relative to the  $^{124}\text{Sn}$  beam will be shown in this paper.

## 2. Results

In this analysis we selected events for which the total charge  $Z_{\text{TOT}}$  and the total parallel momentum are respectively about 70% of the total charge of the colliding system and of the projectile momentum. For this class of events we have plotted in Fig. 1 the atomic number  $Z$  versus parallel velocity of the three heaviest fragments in the events, for three bins of the total charged particle multiplicity  $M$ . These three bins roughly correspond to different windows in a impact parameter scale as can be deduced following prescriptions of Ref. [4], going from semi-peripheral reactions ( $M \leq 6$ ,  $b/b_{\text{max}} > 0.7$ , Fig. 1(a)) to the most dissipative collisions ( $M > 12$ ,  $b/b_{\text{max}} < 0.1$ , Fig. 1(c)). Fig. 1(a) shows clearly that three groups of fragments can be easily separated: fragments originated from a projectile (PLF,  $v_{\text{par}} \approx v_{\text{proj}} = 8$  cm/ns) or target (TLF,  $v_{\text{par}} \approx 1$  cm/ns) remnant, and the class of intermediate velocity fragments at mid-rapidity. By increasing the degree of dissipation of the reaction the three sources of emission, thought more and more blurred, remain evident, indicating a clear persistency of the main binary character of the reaction. In semi-peripheral reactions emissions of intermediate mass fragments in a short time-scale at midrapidity can be mainly attributed to the “neck fragmentation mechanism” [5]: a transient neck structure is formed in a density dilute region at overlapping surfaces of the projectile and target. In Ref. [6] we have introduced a kinematical analysis based on relative velocities between fragments giving the possibility to estimate the time-scale and

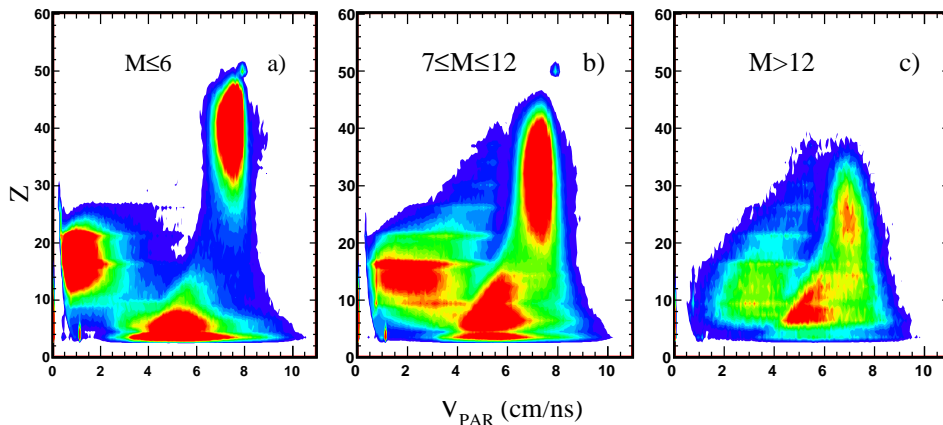


Fig. 1. In the  $^{124}\text{Sn}+^{64}\text{Ni}$  reaction the atomic number  $Z$  of the three heaviest fragments in the event is plotted as a function of the parallel velocity for three different bins of the total charged particles multiplicity  $M$ .

chronology for fragments emission. In the following we extend this method in order to found a correlation between emission time-scale, isotopic contents and angular distributions of the fragments as a function of the degree of dissipation of the reaction.

We sorted the three biggest fragments of the event as a function of the decreasing value of their parallel velocity and we constructed the relative velocities  $V_{\text{REL}}(1,3)$  and  $V_{\text{REL}}(2,3)$  where 1 indicates the velocity of the fastest fragment, 2 the velocity of the slowest one and 3 the velocity of the intermediate one (IVF). The relative velocities were normalised to the velocity corresponding to the Coulomb repulsion energy  $V_{\text{VIOLA}}$  [7]. Fig. 2(a) displays the correlations between the two relative velocities  $r_1 = V_{\text{REL}}/V_{\text{VIOLA}}(1,3)$  and  $r_2 = V_{\text{REL}}/V_{\text{VIOLA}}(2,3)$  for the lowest bin of selected multiplicity. As shown in Ref. [6] this plot gives information on the scenario and time-scale of fragments formation. For less dissipative collisions fragments 1 and 2 are mainly a PLF and a TLF fragments. Intermediate velocity fragments sequentially emitted from a PLF or TLF populate regions along the axes ( $r = 1$ ); particles emitted in a short time-scale and with a  $r_1$  and  $r_2$  simultaneously larger

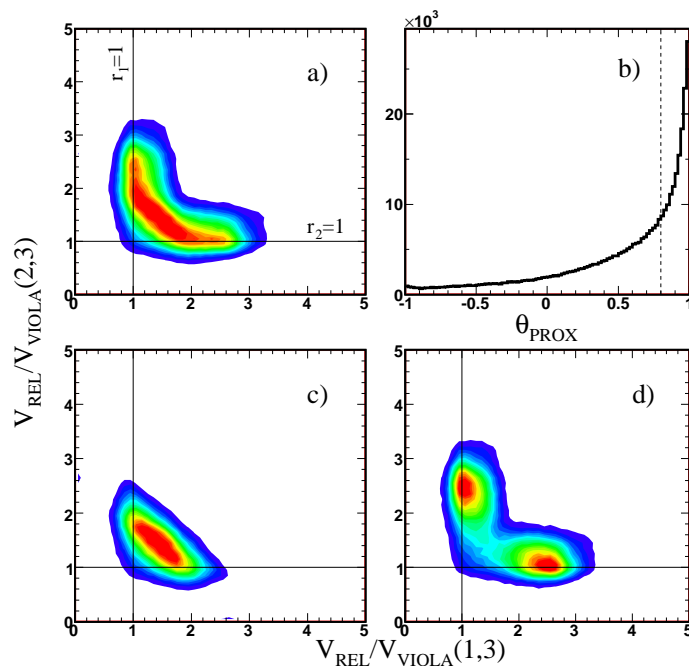


Fig. 2. For the  $^{124}\text{Sn}+^{64}\text{Ni}$  reaction and  $M < 7$  (a) correlations between relative velocities  $V_{\text{REL}}/V_{\text{VIOLA}}$  of the three biggest fragments of the event; (b) distribution of the  $\cos(\theta_{\text{PROX}})$  angle (see text); (c) as (a) but with the condition  $\cos(\theta_{\text{PROX}}) > 0.8$ ; (d) as (a) but with the condition  $\cos(\theta_{\text{PROX}}) \leq 0.8$ .

than 1, characterised by a weak correlation with both PLF and TLF reveal a dynamic origin typical of a neck-fragmentation process [6, 8]. The alignment between PLF-IVF and TLF-IVF represents a good evidence of dynamical origin of mid-rapidity fragments. In Fig. 2(b) is shown the  $\cos(\theta_{\text{PROX}})$  distribution for  $M < 7$  multiplicity bin.  $\theta_{\text{PROX}}$  is the emission angle between the break-up vector (relative velocity between PLF and IVF fragment) and the PLF-TLF separation axis (relative velocity between TLF and PLF-IVF center of mass subsystem) [9]: thus  $\cos(\theta_{\text{PROX}}) = 1$  corresponds to a backward emission respect to the PLF direction. We observe that the distribution of  $\cos(\theta_{\text{PROX}})$  is anisotropic with a marked peak at 1 corresponding to a complete alignment. Fig. 2(c) is obtained selecting  $\cos(\theta_{\text{PROX}}) > 0.8$ . As expected only the zone along the diagonal is populated. On the contrary  $\cos(\theta_{\text{PROX}}) < 0.8$  corresponding to a flat distribution in Fig. 2(b) populates in Fig. 2(d) only the regions along the axis mainly dominated by statistical evaporation from PLF or TLF with no privileged direction for the IVF fragment. This pattern is coherent with the picture of neck dynamics where a collinear neck-like structure is formed between the two main partners of the reaction.

In Ref. [6, 10] it has been shown that it is possible to “calibrate” the time-scale of fragment emission using the correlations discussed before and a simple monodimensional Coulomb trajectory calculation. The light mid-velocity IVFs are produced in a short time (less than 100 fm/c) after the reseparation of the two main partners of the reaction (PLF and TLF). The obtained estimates of the emission times have been found consistent with theoretical calculations describing the IMF emission as the neck fragmentation in stochastic BNV transport model [8]. More recently this prompt emission mechanism has been reproduced in quantum molecular dynamical calculations with the CoMD-II model [11]. Our evaluation is also in agreement with previous simulations based on similar three-body Coulomb trajectory calculations [12].

We now explore the correlations between  $N/Z$  contents, alignments properties and emission time-scale of the intermediate velocity fragments. This kind of correlations as stated in [13] can contribute to disentangle between effects due to isospin dynamics and symmetry term of the EOS from effects that can be merely linked to the accessible phase space in the reaction. Fig. 3 shows the average  $N/Z$  distribution for charge  $Z = 6$  for each compacted bin of the plane  $V_{\text{REL}}(1, 3)$  and  $V_{\text{REL}}(2, 3)$  relative to the  $M \leq 6$  multiplicity bin selection. An interesting correlation is seen: large values of the neutron to proton ratio (neutron enrichment) are mainly produced at the largest Viola deviations, corresponding to the prompt-emission of mid-rapidity source (lowest time-scale emission time) and to the highest degree of alignments. We show in Fig. 4(a), (b) the evolution of relative velocity correlations for

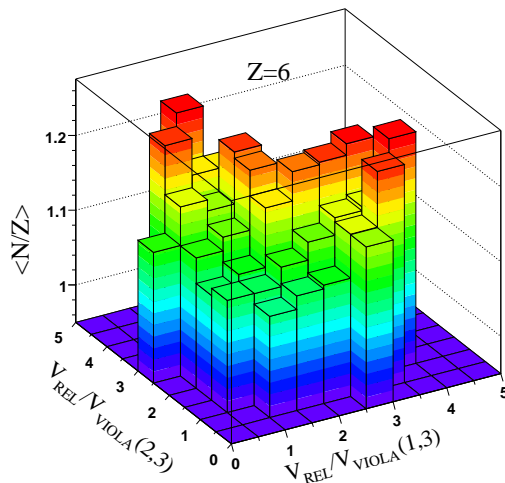


Fig. 3. For the  $^{124}\text{Sn}+^{64}\text{Ni}$  reaction:  $\langle N/Z \rangle$  for charge  $Z = 6$  for different bins in the plane  $V_{\text{REL}}/V_{\text{VIOLA}}(1,3)$ –  $V_{\text{REL}}/V_{\text{VIOLA}}(2,3)$ . Figure refers to  $M < 7$  multiplicity bin.

two different bins in charged particle multiplicity:  $M \leq 6$  (semi-peripheral reactions) and  $M > 12$  (semi-central reactions). On passing from the least to the most dissipative collisions we observe a clear depletion of the region along the axis and an increase of the yield along the first bisector, that shows a pattern very similar to the one predicted by a statistical multifragmentation scenario: in fact, a good quantitative agreement of the centroid of the experimental distribution of Fig. 4(b) is obtained [14] with a statistical multifragmentation model SMM [15] simulation performed under the assumption of a unique source of prompt fragment emission in statistical equilibrium at a low density freeze-out stage. As discussed above, for semi-peripheral reactions the largest values of the  $N/Z$  ratio of the fragments are mainly produced in prompt emission of mid-rapidity source (large Viola deviation in Fig. 3). This is better seen in Fig. 4(c) where the  $\langle N/Z \rangle$  distribution is displayed as a function of charge  $Z$  for the lowest multiplicity bins ( $M \leq 6$ ): full square distribution if obtained for each charge  $Z$  by selecting the highest Viola deviation ( $r > \sim 2$ ) in the  $V_{\text{REL}}/V_{\text{VIOLA}}(1,3)$ –  $V_{\text{REL}}/V_{\text{VIOLA}}(2,3)$  plot, while full circles points correspond to data averaged over the total distribution. Fig. 4(d) shows the same for the most dissipative collisions ( $M > 12$ ).

We observe a “hierarchy” effect in  $N/Z$  distribution: the highest values of  $\langle N/Z \rangle$  are obtained in correspondence of the largest deviation from the Viola velocity ratio (when the short emission time is enforced); at increasing of the violence of the collision the average  $N/Z$  ratio of the fragments tends to become closer to the value obtained averaging over all distribution

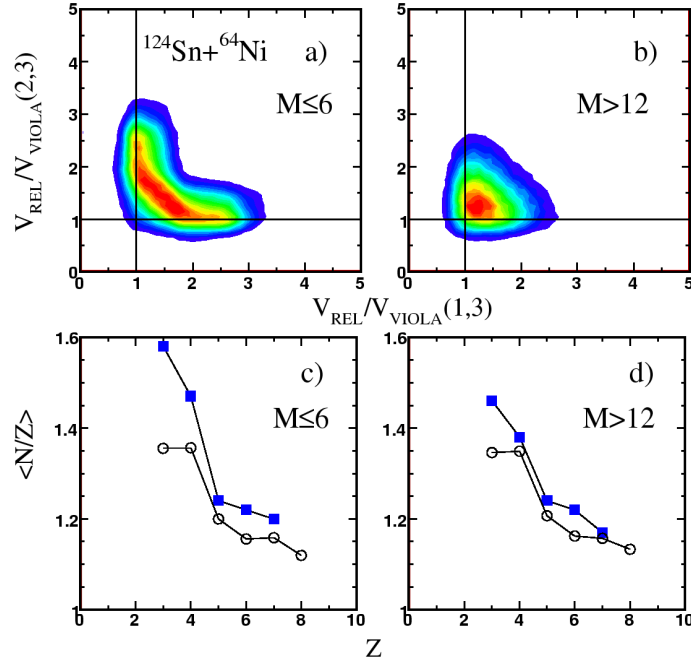


Fig. 4. For the  $^{124}\text{Sn} + ^{64}\text{Ni}$  reaction (top) correlations between relative velocities  $V_{\text{REL}}/V_{\text{VIOLA}}$  of the three biggest fragments in the event for two different bins of the charged particle multiplicity; (bottom) evolution of  $\langle N/Z \rangle$  distribution of the light IVFs as a function of the charge  $Z$  for two different bins of the charged particles multiplicity; full square:  $\langle N/Z \rangle$  obtained imposing a cut on the highest Viola deviations (see text); open circles:  $\langle N/Z \rangle$  averaged on the total distribution.

(full circles), that is relatively independent from the degree of dissipation selection and closer to the natural abundance value. Certainly the different fragments and emission source excitation energies involved play a crucial role in determining this different behaviour. Anyway this is the first attempt to correlate the dependence of the reaction dynamics and reaction time-scales to the isospin observables.

The neutron enrichment of the overlapping region between a projectile-like and target-like fragment at midrapidity has interesting consequences in the study of the reaction dynamics and the density dependence of the symmetry energy: in fact, the neck structure is formed, in a short interaction time, in a dilute region in proximity of the projectile and target remnants at normal density. A migration of neutrons against protons from regions at saturation density to the lower density of the neck zone is expected from microscopic transport models [8]. Thus *neck fragmentation* is an important observable to probe the symmetry energy around saturation density.

In order to better disentangle this point we have correlated the alignment between PLF,IVF and TLF for the  $M \leq 6$  multiplicity bin with the  $\langle N/Z \rangle$  of the IVFs. We have constructed event-by-event the  $\phi$ -plane angle defined as the angle between the PLF-TLF separation axis and the projection of the IVF-PLF relative velocity axis onto the reaction plane (see Ref. [16]). A  $\phi$ -plane  $\approx 0$  corresponds to the maximum degree of alignment while sequential emission produces a flat  $\phi$ -plane distribution. Fig. 5(a) shows the  $\langle N/Z \rangle$  as a function of the  $\phi$ -plane for IVFs with charge  $3 \leq Z \leq 9$ . When dynamical emitted IVFs are selected a relatively narrow distribution with  $\langle N/Z \rangle$  centered around  $\phi$ -plane  $\approx 0$  is obtained (full circles). Averaging over all events (sequential+prompt emission) one observes a wider distribution (histogram). Fig. 5(b) shows a simulation for the same system using the stochastic transport equation of Ref. [8] for two different choices of the symmetry energy [17]. We note that the  $\langle N/Z \rangle$  decreases as a function of the  $\phi$ -plane for the asy-stiff case while the correlation becomes flatter for the asy-soft case. Qualitative comparison with the experimental data shows a better agreement with the “stiff” behaviour of the symmetry energy. Also if influence of sequential decay in primary fragments is not taken into account in the present simulation, comparison between experimental and theoretical data shows a first evidence of the influence of the symmetry energy term at a density slightly lower than the saturation one.

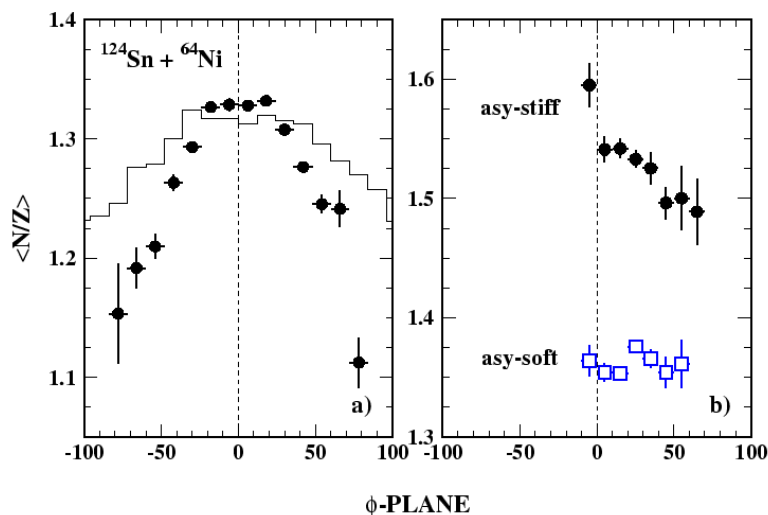


Fig. 5. (a) Experimental (for  $M \leq 6$  multiplicity bin)  $\langle N/Z \rangle$  as a function of the  $\phi$ -plane angle for IVF of charge  $3 \leq Z \leq 9$ . Points: prompted emitted particle selection; histogram:  $\langle N/Z \rangle$  averaged on the total distribution. (b) Stochastic BNV simulation; square: asy-soft; circles: asy-stiff symmetry term of EOS.



### 3. Conclusions

With the Chimera multidetector we have explored fragment formation processes in a wide “time” range from prompt to sequential emission. An analysis method, based upon correlations between relative velocities of IMF’s respect to projectile-like or target-like fragments, gives information on time sequence and time scale of the emission pattern of fragment production. Based essentially on final state (Coulomb) interaction, the method can probe the basic physical assumptions of dynamical models in heavy ions collisions. We have shown that the fragments  $N/Z$  ratio can be correlated with fragments emission time. Indeed correlations between fragments kinematical properties (velocities, alignments, angular distributions) and their  $N/Z$  show strong sensitivity of the isospin degree of freedom to the chronology of fragment formation. Large value of  $N/Z$  have been measured for those fragments produced in the early stage of the collisions. With increasing of the violence of the collision we observe a transition from peripheral collisions where coexistence of prompt emission and sequential decay is progressively suppressed towards a scenario dominated by a prompt multifragment decay.

### REFERENCES

- [1] For a recent review see for example: M. Colonna, M.B. Tsang, *Eur. Phys. J.* **A30**, 165 (2006); V. Baran, M. Colonna, V. Greco, M. Di Toro, *Phys. Rep.* **410**, 335 (2005); Bao-An Li, L.W. Chen, C.M. Ko, *Phys. Rep.* **464**, 113 (2008).
- [2] A. Pagano *et al.*, *Nucl. Phys.* **A734**, 504 (2004).
- [3] E. Geraci *et al.*, *Nucl. Phys.* **A732**, 173 (2004).
- [4] C. Cavata *et al.*, *Phys. Rev.* **C42**, 1760 (1990).
- [5] M. Di Toro, A. Olmi, R. Roy, *Eur. Phys. J.* **A30**, 65 (2006).
- [6] E. De Filippo *et al.*, *Phys. Rev.* **C71**, 044602 (2005).
- [7] D.J. Hinde *et al.*, *Nucl. Phys.* **A472**, 318 (1987).
- [8] V. Baran *et al.*, *Nucl. Phys.* **A730**, 329 (2004).
- [9] F. Bocage *et al.*, *Nucl. Phys.* **A676**, 391 (2000).
- [10] J. Wilczyński *et al.*, *Int. J. Mod. Phys.* **E14**, 353 (2005).
- [11] M. Papa *et al.*, *Phys. Rev.* **C75**, 054616 (2007).
- [12] S. Piantelli *et al.*, *Phys. Rev. Lett.* **88**, 052701 (2002).
- [13] R. Lioni *et al.*, *Phys. Lett.* **B625**, 33 (2005).
- [14] P. Russotto *et al.*, Proceedings of the INPC 2007 Conference, Tokio, June 3–8 2007, Vol. II, p. 507, eds. S. Nagamiya, T. Motobayashi, M. Oka, R.S. Hayano, T. Nagae, 2008.
- [15] J. Bondorf, A.S. Botvina *et al.*, *Phys. Rep.* **257**, 133 (1995).
- [16] E. De Filippo *et al.*, *Phys. Rev.* **C71**, 064604 (2005).
- [17] M. Di Toro *et al.*, Proceedings of the IWM2007 Int. Workshop on Multifragmentation, Caen, 4–7 Nov. 2007, SIF Conf. Proc. vol. 95, p. 183, 2008.